Study of vector-meson production in e^+e^- annihilation at $\sqrt{s}=29$ GeV

S. Abachi,* M. Derrick, P. Kooijman,† B. Musgrave, L. E. Price, J. Repond, K. Sugano, and P. Waschbusch
Argonne National Laboratory, Argonne, Illinois 60439

D. Blockus, B. Brabson, J-M. Brom,‡ C. Jung,§ H. Ogren, and D. R. Rust
Indiana University, Bloomington, Indiana 47405

C. Akerlof, J. Chapman, D. Errede,** M. T. Ken, D. I. Meyer, H. Neal, D. Nitz, R. Thun, and R. Tschirhart*
University of Michigan, Ann Arbor, Michigan 48109

P. Baringer,†† B. G. Bylsma,‡‡ R. DeBonte, D. Koltick, E. H. Low,§§ R. L. McIlwain, D. H. Miller, C. R. Ng, and E. I. Shibata
Purdue University, West Lafayette, Indiana 47409

B. Cork
Lawrence Berkeley Laboratory, Berkeley, California 94720
(Received 14 February 1989)

This paper reports cross-section measurements for the ρ^0 and $K^*(890)$ vector mesons produced in e^+e^- annihilation at $\sqrt{s}=29$ GeV. The data, which were taken with the High Resolution Spectrometer operating at the SLAC colliding-beam facility PEP, correspond to an integrated luminosity of 291 pb^{-1}. The measured multiplicities for fractional momentum $x>0.05$ are $N_{\rho^0}=0.79\pm0.04$ and $N_{K^{*0}(890)}=0.53\pm0.04$. The measured fragmentation functions agree well with the predictions of the Lund model and when extrapolated to threshold, the corresponding total multiplicities are $N_{\rho^0}=0.90\pm0.05$ and $N_{K^{*0}(890)}=0.59\pm0.05$.

INTRODUCTION

High-energy e^+e^- annihilation provides the simplest laboratory for studying the transformation of quarks and gluons into hadrons. The center-of-mass energy is known and it is shared by a few partons, either by a $q\bar{q}$ pair or a $q\bar{q}$ pair plus a small number of gluons. In addition, the $q\bar{q}$ pairs of different flavor are produced in a known ratio.

Although, in principle, the parton-level processes can be calculated within QCD, the transformation of the partons into hadrons is both nonperturbative and complex. Much of the effort in this subject has, therefore, been directed at using the data to parametrize these transitions in the context of one of the available fragmentation models.[1–3]

In these models one of the unknowns is the probability that a quark-antiquark pair produce a vector meson as compared to its pseudoscalar partner. Although this ratio arises naturally from the cluster[2] and string[3] ideas, the results are still dependent on unknown parameters. It is thus important to measure and compare the production rates of vector and pseudoscalar mesons for all quark flavors.

Several such measurements for the u, d, and s quarks giving ρ^0 and $K^{*0}(890)$ mesons have been reported from studies of continuum e^+e^- annihilation at center-of-mass energies near 10 GeV by the CLEO and ARGUS Collaborations[4] as well as from the groups[5] working at the SLAC storage ring PEP operating at 29 GeV. Similar results[6] at a somewhat higher energy are available from the collaborations working at the DESY storage ring PETRA.

We have previously reported measurements[7] of ρ^0 and K^{*0} production based on an initial data sample of 185 pb^{-1}. In this paper we present our final measurements, which come from the full event sample, corresponding to an integrated luminosity of 291 pb^{-1}. We have already published equivalent data for $K^{*\pm}(890)$ production,[8] as well as the production cross sections[9] for the tensor mesons $f_2(1270)$ and $K^*(1430)$.

EXPERIMENTAL DETAILS

The High Resolution Spectrometer (HRS) was operated at the 29-GeV e^+e^- storage ring PEP. For the full data taking, the HRS was equipped with tracking devices consisting of 17 layers of drift chambers surrounded by lead-scintillator shower counters. Both systems covered 90% of the solid angle, and were contained in a 16.2-kG solenoidal magnetic field of 4.5 m diameter. The spectrometer provided excellent momentum resolution for the charged tracks over the full solid angle:

$\Delta p_t/p_t = (0.2p_t\%)$ (p_t in GeV/c), where p_t is the momentum component perpendicular to the e^+e^- beam axis. The resulting two-particle mass resolution was typically 15 MeV for the momentum and mass ranges covered by these measurements.

Identification of a charged track as a π, K, or p was only possible at low momentum using the time-of-flight information from the shower counters. However, this limited information was not used in the present analysis. A detailed description of the detector and of the hadronic event selection have been reported elsewhere.[10]

This analysis used a clean sample of hadronic events that contained high-quality tracks originating from the primary vertex of the annihilation. Each event was required to have a sum of visible energy, both charged and neutral, of at least 10 GeV. Events with fewer than five reconstructed charged tracks were rejected. In all the remaining events, tracks were removed from this analysis if they failed to register in more than 60% of the drift-chamber layers available to them, of if they formed an angle (θ) with respect to the beam direction such that $|\cos\theta| > 0.9$. Finally, it was required that p_t exceed 0.125 GeV/c.

Since this experiment rests on the analysis of two-particle mass combinations, it is important to use a sample of high-quality tracks. Our analysis of the charged-particle multiplicity distributions[11] shows that the above selections satisfy this need. The selections also allow a reliable simulation of the experiment, which is necessary in calculating the acceptance. The data sample consists of $\sim 100\,000$ events with a background, primarily from two-photon annihilation, of a few percent.

ANALYSIS TECHNIQUE

Since no particle identification was used, all tracks passing the above cuts were considered in turn as pion and kaon candidates and were used to calculate the $\pi^+\pi^-$ and $K^\pm\pi^\mp$ invariant masses. The doubly charged $\pi^\pm\pi^\mp$ and $K^\pm\pi^\pm$ spectra were also generated and are shown in Fig. 1. These doubly charged spectra were subtracted, bin by bin, from the corresponding neutral charge combinations. This technique is a simple way of removing most of the combinational background. Figures 2 and 3 show the resulting subtracted spectra for $\pi^+\pi^-$ and $K^\pm K^\mp$, respectively. The selection $x > 0.05$, where $x = p/p_{\text{beam}}$ is the fractional momentum of the two-particle system, has been imposed on the data shown in Figs. 1–3 to reduce the combinatorial background.

The $\pi^+\pi^-$ spectrum of Fig. 2 shows several features: a shoulder just below 400 MeV that comes from the decays $\eta^0 \to \pi^+\pi^-\pi^0$; a broad peak from threshold to about 650 MeV coming from the $\omega^0 \to \pi^+\pi^-\pi^0$ decays; a narrow peak near 500 MeV corresponding to the $K_S^0 \to \pi^+\pi^-$ decays; an excess near 1 GeV that we have identified[9] with the $f_0 \to \pi^+\pi^-$ decays; and an enhancement in the ρ^0 mass region. This peak includes K^{*0} decays with the charged K mesons incorrectly assigned to the pion mass, in addition to the true $\rho^0 \to \pi^+\pi^-$ decays.

The $K^\pm\pi^\mp$ spectrum of Fig. 3 is simpler: the prominent feature is the peak at 900 MeV coming from the $K^{*0} \to K^\pm\pi^\mp$ decays. In addition, there are shoulders below and above this region coming from $K^0 \to \pi^+\pi^-$ and $\rho^0 \to \pi^+\pi^-$ decays misidentified as $\pi^\pm K^\mp$ combinations. The spectrum also includes K^{*0} decays in which the K and π are interchanged, as well as $\omega^0 \to \pi^+\pi^-\pi^0$ decays where one charged pion is misidentified as a kaon.

To determine the contributions of the ρ^0 and K^{*0}, these spectra were fitted to the sum of several components. The first contributions were smooth combinatorial backgrounds, shown by the dashed lines, using the functional form

$$F(m) = \alpha_0(m - m_0)^{\alpha_1}\exp(\alpha_2 m + \alpha_3 m^2)\,, \tag{1}$$

where the α_n's are free parameters and m_0 is the appropriate $\pi\pi$ or $K\pi$ mass threshold. This form also gives good fits to the doubly charged spectra, as seen by the lines in Fig. 1. The data and this combinatorial background refer to the ordinate scale on the left in Figs. 2 and 3. Additional contributions from η^0 decays (light-dotted line) and ω^0 decays (heavy-dotted line) were also

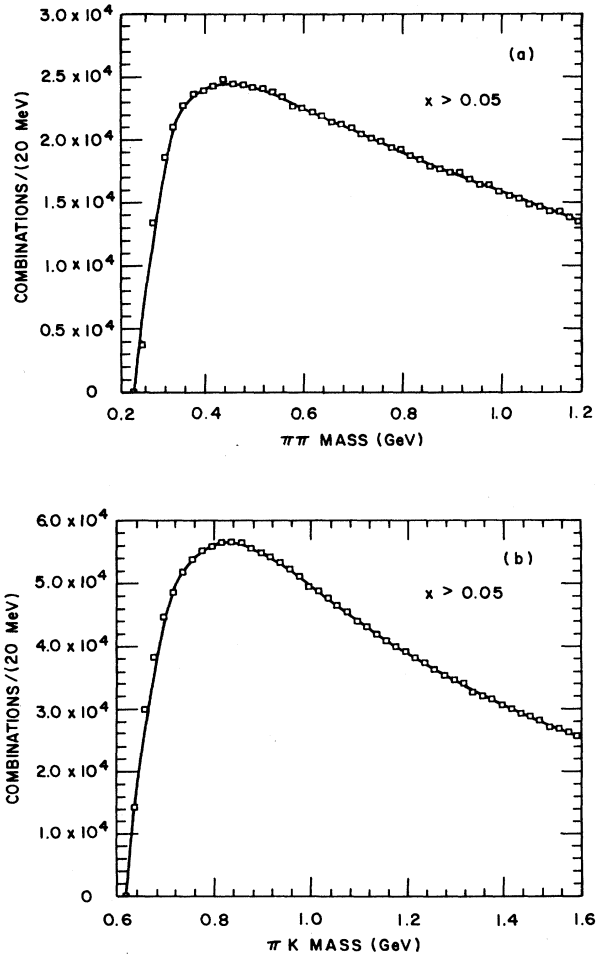

FIG. 1. Doubly charged mass spectra for $x > 0.05$, (a) $\pi^\pm\pi^\pm$, (b) $\pi^\pm K^\pm$. The lines show fits to the form $F(m) = \alpha_0(m - m_0)^{\alpha_1}\exp(\alpha_2 m + \alpha_3 m^2)$.

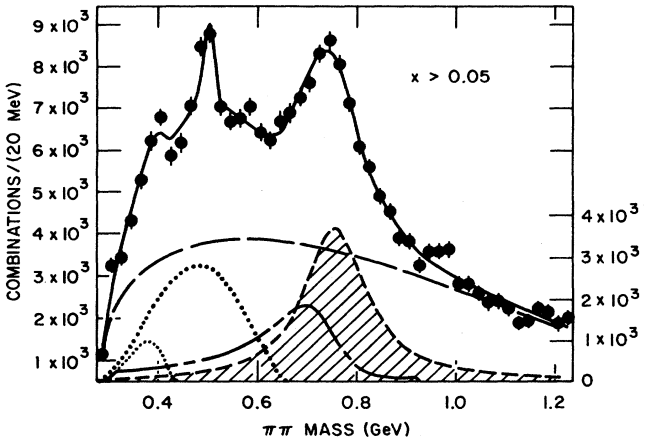

FIG. 2. Subtracted neutral $\pi^+\pi^-$ mass spectrum for $x > 0.05$. The dashed line shows the smooth background using the form given in Eq. (1) of the text. This function also well represents the doubly charged spectra. The data, the total fit, and the above background contribution refer to the ordinate scale on the left. Four other individual contributions to the fit are shown at the bottom of the figure with ordinate scale on the right. (i) Contribution from $\eta^0\to\pi^+\pi^-\pi^0(\gamma)$ decays (light-dotted line); (ii) contribution from $\omega^0\to\pi^+\pi^-\pi^0(\gamma)$ decays (heavy-dotted line); (iii) K^{*0} reflection (short-dashed–long-dashed line); (iv) ρ^0 contribution (hatched area). The fit also includes a contribution from $K^0\to\pi^+\pi^-$ decays where the decay occurs close to the primary vertex.

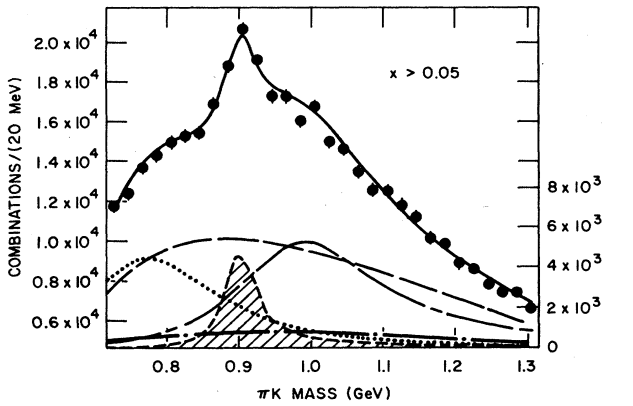

FIG. 3. Subtracted neutral $\pi^\pm K^\mp$ mass spectrum for $x > 0.05$. The dashed line shows the smooth background using the form given in Eq. (1) of the text. This function also well represents the doubly charged spectra. The data, the total fit, and the above background contribution refer to the ordinate scale on the left. Four other individual contributions to the fit are shown at the bottom of the figure with ordinate scale on the right. (i) Contribution from $\omega^0\to\pi^+\pi^-\pi^0$ with a $\pi^\pm$ misidentified as a $K^\pm$ (heavy-dotted line); (ii) ρ^0 reflection (short-dashed–long-dashed line); (iii) K^{*0} reflection with $K^\pm\leftrightarrow\pi^\pm$ interchanged (dashed-dotted line); (iv) K^{*0} contribution (hatched area). The fit also includes a contribution from $K^0\to\pi^+\pi^-$ decays with a charged pion incorrectly assigned the kaon mass.

included. The ω^0 rate was fixed to be equal to that of the ρ^0 and the η^0 production cross section was taken from our measurements.[12] The K^{*0} and ρ^0 reflections resulting from the fits are shown by the long-dashed–short-dashed lines, and the K^{*0} reflection resulting from the $K^\pm\leftrightarrow\pi^\pm$ interchange is shown as the dashed-dotted line in Fig. 3. These contributions refer to the ordinate scales on the right. The contribution from the $K_S^0\to\pi^+\pi^-$ decays were measured from the data of Fig. 2. The reflected spectra were reconstructed from the pure resonance samples generated with the Lund Monte Carlo program[3] (version 6.3) and processed through the full detector simulation, including all analysis cuts. The fits were done simultaneously to the $\pi\pi$, and $K\pi$ spectra and gave a mean χ^2 per degree of freedom of 0.8.

The fitted ρ^0 and K^{*0} contributions, which are shown as hatched areas in Figs. 2 and 3, were parametrized by

$$F(m)=\frac{2}{\pi}\frac{mm_R\Gamma}{(m^2-m_R^2)^2+m_R^2\Gamma^2}\ , \tag{2}$$

$$\Gamma=\Gamma_R\left[\frac{q}{q_R}\right]^3\frac{m_R}{m}\ , \tag{3}$$

where m_R and Γ_R are the resonance masses and widths, and q is the $\pi(K)$ momentum in the resonance rest frame; $q=q_R$ when $m=m_R$. In doing these fits, the resonance masses and widths of the ρ^0 and K^{*0} meson were fixed at their accepted values.[13] The shapes of the other contributions, shown by the lines in Figs. 2 and 3 and discussed above, were fixed by the Monte Carlo simulation. The er-

TABLE I. ρ^0 cross sections.

Z selection	Number of events	Cross section $\frac{s}{\beta}\frac{d\sigma}{dZ}$ (μb GeV^2)
0.082	7186	2.52±0.53
0.103	5507	1.57±0.33
0.125	4611	1.25±0.24
0.147	4579	1.08±0.18
0.171	3832	0.81±0.17
0.195	3033	0.68±0.14
0.219	2950	0.49±0.11
0.243	2852	0.51±0.07
0.268	2147	0.47±0.07
0.292	1726	0.38±0.06
0.317	1434	0.32±0.06
0.342	1034	0.23±0.05
0.366	906	0.20±0.04
0.391	975	0.22±0.06
0.416	833	0.11±0.03
0.441	791	0.09±0.02
0.478	787	0.08±0.02
0.553	743	0.040±0.015
0.652	303	0.016±0.005
0.752	271	0.014±0.005
0.852	118	0.006±0.003

TABLE II. $K^*(890)$ cross sections.

	K^{*0}		$K^{*\pm}$	
Z selection	Number of events	Cross section $\frac{s}{\beta}\frac{d\sigma}{dZ}$ (μb GeV^2)	Number of events	Cross section $\frac{s}{\beta}\frac{d\sigma}{dZ}$ (μb GeV^2)
0.098	2704	1.51±0.41	200	1.96±0.53
0.140	2216	0.87±0.17	491	1.12±0.22
0.186	1457	0.49±0.20	199	0.63±0.15
0.233	996	0.30±0.07	144	0.39±0.09
0.282	881	0.25±0.05	132	0.32±0.07
0.331	879	0.23±0.05	124	0.30±0.07
0.380	581	0.15±0.024	89	0.19±0.03
0.430	329	0.08±0.02	51	0.10±0.03
0.480	362	0.08±0.02	53	0.11±0.02
0.554	360	0.04±0.01	59	0.05±0.01
0.653	139	0.015±0.006	24	0.019±0.008
0.802	77	0.004±0.002	12	0.005±0.002

rors on the ρ^0 and K^{*0} resonance contributions were obtained by looking for a unit change in χ^2 of the fits, as well as by varying the contributions of the other resonances (η,ω,K^0) within their errors.

Similar fits were done with different x selections, and the resulting event numbers and cross sections expressed as $(s/\beta)(d\sigma/dZ)$ are given in Tables I and II. In calculating Z, the fractional energy of the meson ($Z=2E_{\text{meson}}/\sqrt{s}$), we use $\sqrt{s}=29$ GeV, whereas for s we use the square of 28.3 GeV since this is the mean event energy after initial-state electromagnetic radiation. The normalization of the cross section comes from a study of wide-angle Bhabha-scattering events, which gave an integrated luminosity for the experiment of 291±7 pb^{-1}.

The integral of the data from $x=0.5$ to $x=1$ gives overall multiplicities per event in this kinematic range of 0.79±0.04 ρ^0 and 0.53±0.04 $K^{*0}(890)$. These values are independent of any fragmentation model. In order to determine the total multiplicities, an extrapolation to threshold is necessary. To do this, we use the shape given by the Lund model. Figures 4 and 5 show the invariant cross sections as a function of the fractional energy variable Z. The lines are the predictions of the Lund model fitted to the data above $x=0.05$. Extrapolating to threshold using these curves yields overall multiplicities of 0.90±0.05 ρ^0 and 0.59±0.05 $K^{*0}(890)$ particles per event to be compared to 0.89 ρ^0 and 0.62 K^{*0} given by version 6.3 of this model.

The resulting total cross sections, R values, and mean multiplicities are summarized in Table III. The R value is the ratio of the measured cross section to the point cross section, and in this calculation we use 28.3 GeV as the mean energy of an annihilation event. The values of $\langle n\rangle_{\rho^0}=0.90\pm0.05$ ($\langle n\rangle_{K^{*0}}=0.59\pm0.05$) may be compared with our previous measurements of $\langle n\rangle_{\rho^0}=0.95\pm0.09$ ($\langle n\rangle_{K^{*0}}=0.63\pm0.10$), based on a subset of the present data.[7]

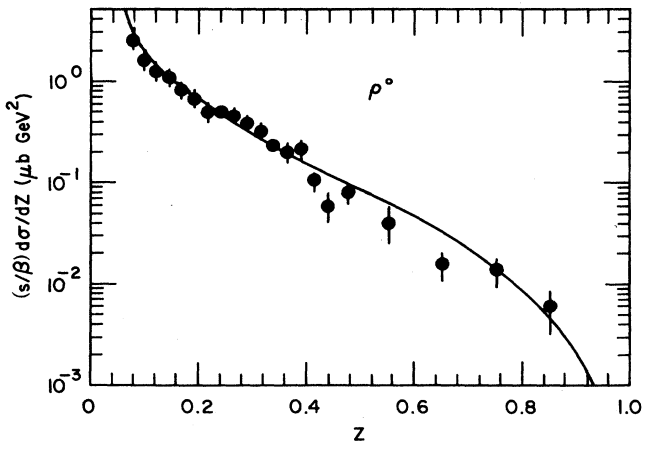

FIG. 4. Fragmentation cross section $[(s/\beta)d\sigma/dZ$ (μb GeV^2)] for ρ^0 production as measured in this experiment. The line shows the prediction of the Lund model.

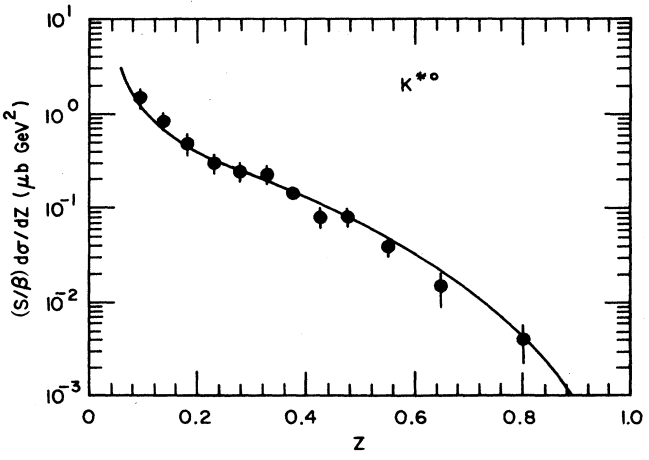

FIG. 5. Fragmentation cross section $[(s/\beta)d\sigma/dZ$ (μb GeV^2)] for K^{*0} production as measured in this experiment. The line shows the prediction of the Lund model.

TABLE III. Vector-meson cross sections.

Meson	Cross section (pb)	R value	Mean multiplicity
ρ^0	360±20	3.09±0.17	0.90±0.05
$K^{*0}(890)$	236±20	2.02±0.17	0.59±0.05

Figure 6 compares our cross sections to previous measurements by other collaborations.[5,6] Again, the agreement, both in the shape and in the normalization of the fragmentation functions, is reasonable, particularly for the $K^{*0}(890)$. Our data extend the measurements to higher-Z values.

The mean multiplicities reported by the PEP and PETRA Collaborations are summarized in Table IV. The values reported by the different groups are in good agreement. We also show in Table IV our measurement of the multiplicity of the charged $K^*(890)$. The value of $\langle n \rangle_{K^{*\pm}} = 0.62 \pm 0.045 \pm 0.04$ agrees within errors with the mean multiplicity measured for the neutral $K^*(890)$.

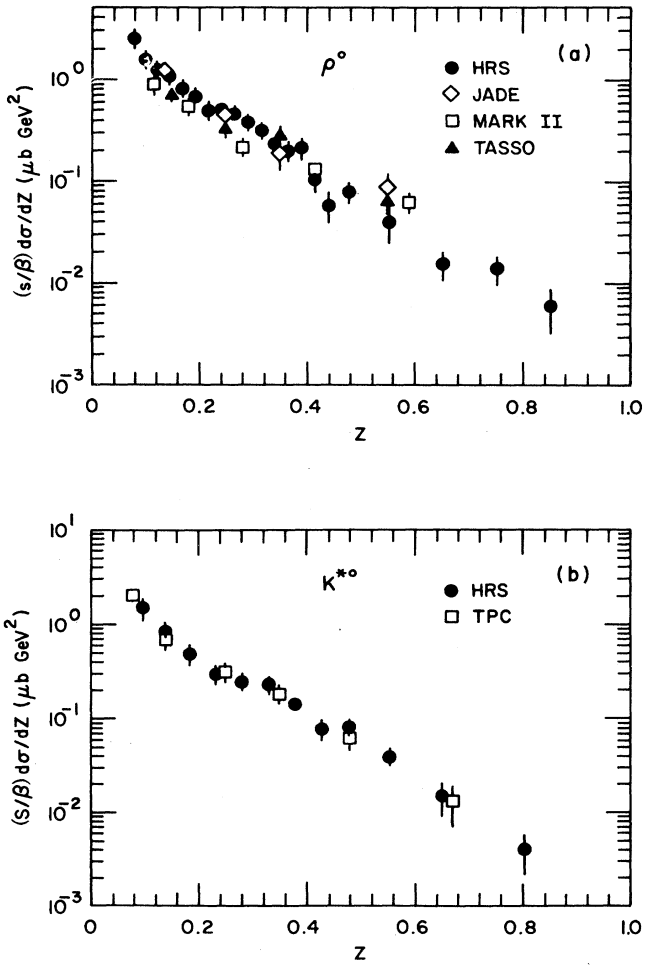

FIG. 6. Comparison of cross-section measurements near $\sqrt{s} = 30$ GeV for (a) ρ^0 production, (b) K^{*0} production.

TABLE IV. Multiplicities of ρ^0 and $K^{*0}(890)$ in e^+e^- annihilation near 30 GeV.

Meson	Mean number per event	Detector	Reference
ρ^0	0.73±0.06	TASSO	6
	0.98±0.09 ±0.15	JADE	6
	0.90±0.05	HRS	This expt.
K^{*0}	0.87±0.16 ±0.08	JADE	6
	0.49±0.04 ±0.07	TPC	5
	0.59±0.05	HRS	This expt.
$K^{*\pm}$	0.62±0.045±0.04	HRS	8

DISCUSSION OF RESULTS

There is quite good agreement, both in normalization and shape, between our data and the Lund model, as shown by the comparisons in Figs. 4 and 5. This is to be expected as the model has been tuned to fit similar data published earlier. The data for $Z \gtrsim 0.4$, however, do tend to lie below the curve. This is also the case with our measurements of η^0 (Ref. 12) and ϕ (Ref. 14) production. Such a systematic difference probably comes from the neglect of high-mass states that, in turn, decay to the states being measured. For example, ρ^0 mesons from the decay $a_1 \rightarrow \rho\pi$ are not included in the Lund model.

The Lund model has many free parameters and the $K^*(890)$ curve, shown in Fig. 5, was calculated with a strange-quark suppression factor γ_s of 0.34. In the con-

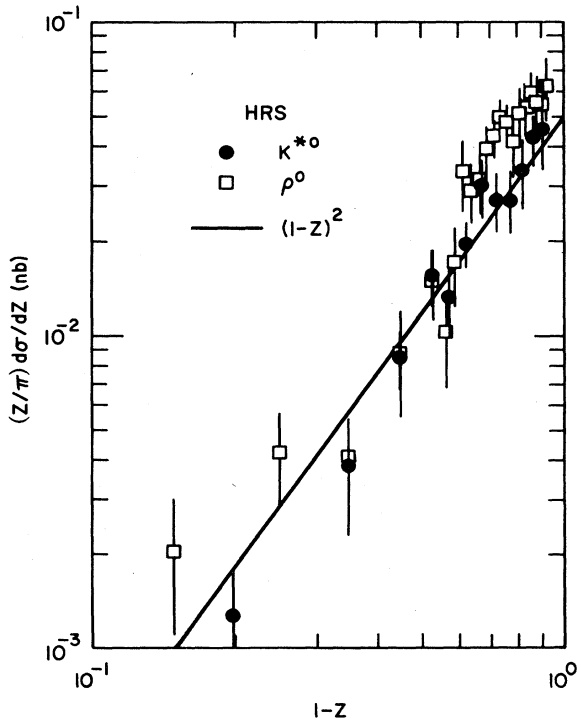

FIG. 7. Invariant cross sections for vector-meson production compared to a $(1-Z)^2$ variation expected for first-order quark-meson transitions.

text of current ideas this suppression arises because of the higher mass of the s quark relative to the u and d quarks. The parameter γ_s is the ratio of the probabilities of making an $s\bar{s}$ pair relative to a $u\bar{u}$ or $d\bar{d}$ pair in the fragmentation chain and so is, in principle, measured by the $K^*(890)/\rho$ ratio.

To determine γ_s, it is necessary to subtract the number of vector mesons that come from decays of higher-mass states such as the D mesons and the $K^*(1430)$ in order to estimate the direct production of vector mesons. The systematic uncertainties in this technique are difficult to estimate, but the e^+e^- experiments are consistent with $\gamma_s = 0.33 \pm 0.03$ (Ref. 15).

An alternative method would be to use the data at high Z where the direct production will dominate. From the leading quarks, the relative production rates of the ρ^0 and K^* mesons, assuming $\sigma(\omega^0) = \sigma(\rho^0)$, are

$$\rho^0 : K^{*0} : K^{*\pm} :: 2.5 f_V^{u,d} : f_V^s (1+\gamma_s) : f_V^s (1+4\gamma_s) , \quad (4)$$

where f_V is the probability of producing a vector meson from the $q\bar{q}$ pair that includes the leading quark. The ratio of the directly produced neutral-to-charged K^* mesons, therefore, directly measures γ_s, and for $\gamma_s = \frac{1}{3}$ this ratio should be $\frac{4}{7}$. In addition, the invariant cross section should, on dimensional counting arguments, show a $(1-Z)^2$ behavior for a first-order quark-meson transition.[16] The data of Table I show a somewhat smaller cross section for K^{*0} production as compared to $K^{*\pm}$, and the invariant cross sections, shown in Fig. 7, are consistent with a $(1-Z)^2$ behavior within the large errors.

These first-order transitions from the leading quark should dominate for $Z > 0.8$; below this value, higher-order transitions become increasingly more important, resulting in a sharpening of the Z behavior. Because the higher-order fragmentation is symmetric for K^{*0} and $K^{*\pm}$, there is an increase of the predicted $K^{*0}/K^{*\pm}$ ratio from 0.57 to, for example, 0.74 for $Z > 0.5$ with $\gamma_s = \frac{1}{3}$. Contributions from cascade decays of heavier strange mesons, such as the $K^*(1430)$, are negligible due to the low production cross section, and decays of charmed mesons only populate the region below $Z = 0.5$. The measured $K^{*0}/K^{*\pm}$ ratio is 0.95 ± 0.12, somewhat higher than the 0.74 expected.

The cross section ratio for ρ^0/K^{*0} production above $Z = 0.5$ is 1.49 ± 0.13 which gives $f_V^{u,d}/f_V^s = 0.79 \pm 0.07$, again assuming $\gamma_s = \frac{1}{3}$. The relatively smaller probability of producing a vector meson from the u and d quarks, as compared to the s quark, is expected from the small π/ρ mass ratio as compared to that for the K/K^*. Clearly higher statistics data are required for a more quantitative study of these issues.

ACKNOWLEDGMENTS

We wish to convey our gratitude to the SLAC cryogenic group and the technical staffs of PEP and the collaborating institutions, whose important contributions made this experiment possible. This work was supported in part by the U.S. Department of Energy, under Contracts Nos. W-31-109-ENG-38, DE-AC02-76ER01112, DE-AC03-76SF00098, DE-AC02-76ER01428, and DE-AC02-84ER40125.

*Present address: Fermi National Accelerator Laboratory, Batavia, IL 60510.
†Present address: NIKHEF-H, Amsterdam, The Netherlands.
‡Present address: CRN Division de Hautes Energies, Strasbourg, France.
§Present address: Stanford Linear Accelerator Center, Stanford, CA 94305.
**Present address: University of Wisconsin, Madison, WI 53706.
††Present address: University of Kansas, Lawrence, KS 66045.
‡‡Present address: Ohio State University, Columbus, OH 43210.
§§Present address: Virginia Polytechnic Institute and State University, Blacksburg, VA 24061.

[1]P. Hoyer *et al.*, Nucl. Phys. **B161**, 149 (1979); A. Ali *et al.*, Phys. Lett. **93B**, 155 (1980).
[2]R. D. Field and S. Wolfram, Nucl. Phys. **B213**, 65 (1983); B. R. Webber, *ibid.* **B238**, 492 (1984); T. D. Gottschalk, *ibid.* **B239**, 325 (1984); T. D. Gottschalk and D. Morris, *ibid.* **B288**, 729 (1987).
[3]B. Andersson, G. Gustafson, and T. Sjostrand, Phys. Rep. **97**, 32 (1983).
[4]CLEO Collaboration, S. Behrends *et al.*, Phys. Rev. D **31**, 2161 (1985); ARGUS Collaboartion, H. Albrecht *et al.*, Phys. Lett. B **183**, 419 (1983).
[5]TPC Collaboration, H. Aihara *et al.*, Phys. Rev. Lett. **53**, 2378 (1984). The K^{*0} data of the TPC Collaboration uses energy-loss measurements to separate $\pi^\pm$ from $K^\pm$ so that the combinatorial background is minimized and the resulting cross-section errors, shown in Fig. 6(b), are comparable to ours even though the TPC integrated luminosity is 77 pb^{-1}.
[6]TASSO Collaboration, W. Brandelik *et al.*, Phys. Lett. **117B**, 135 (1982); JADE Collaboration, W. Bartel *et al.*, *ibid.* **145B**, 441 (1985).
[7]M. Derrick *et al.*, Phys. Lett. **158B**, 519 (1985). The data selections used in this work were somewhat different from those used in the present analysis. In particular, the track selection used previously included a larger fraction of the $K^0 \to \pi^+\pi^-$ decays.
[8]S. Abachi *et al.*, Phys. Lett. B **199**, 151 (1987).
[9]S. Abachi *et al.*, Phys. Rev. Lett. **57**, 1990 (1986).
[10]D. Bender *et al.*, Phys. Rev. D **30**, 515 (1984); **31**, 1 (1985).
[11]M. Derrick *et al.*, Phys. Rev. D **34**, 3304 (1986).
[12]S. Abachi *et al.*, Phys. Lett. B **205**, 111 (1988).
[13]Particle Data Group, G. P. Yost *et al.*, Phys. Lett. B **204**, 1 (1988).
[14]M. Derrick *et al.*, Phys. Rev. Lett. **54**, 2568 (1985).
[15]M. Derrick and S. Abachi, in *Review Volume on Hadronic Multiparticle Production,* edited by P. Carruthers (World Scientific, Singapore, 1988).
[16]M. Derrick *et al.*, Phys. Lett. **164B**, 199 (1985).